

Article

Insights into the SAM Synthetase Gene Family and Its Roles in Tomato Seedlings under Abiotic Stresses and Hormone Treatments

Parviz Heidari ^{1,*}, Faezeh Mazloomi ¹, Thomas Nussbaumer ² and Gianni Barcaccia ³

¹ Faculty of Agriculture, Shahrood University of Technology, Shahrood 3619995161, Iran; faezeh_mazloomi@yahoo.com

² Helmholtz Zentrum München, Deutsches Forschungszentrum für Gesundheit und Umwelt (GmbH), 85764 Neuherberg, Germany; thomasnbionf@gmail.com

³ Laboratory of Genomics for Breeding, DAFNAE, University of Padova, Campus of Agripolis, 35030 Legnaro, Italy; gianni.barcaccia@unipd.it

* Correspondence: heidarip@shahroodut.ac.ir; Tel.: +98-912-0734-034

Received: 4 April 2020; Accepted: 27 April 2020; Published: 4 May 2020



Abstract: S-Adenosyl-L-methionine (SAM) is a key enzyme involved in many important biological processes, such as ethylene and polyamine biosynthesis, transmethylation, and transsulfuration. Here, the SAM synthetase (SAMS) gene family was studied in ten different plants (*Arabidopsis*, tomato, eggplant, sunflower, *Medicago truncatula*, soybean, rice, barley, *Triticum urartu* and sorghum) with respect to its physical structure, physicochemical characteristics, and post-transcriptional and post-translational modifications. Additionally, the expression patterns of SAMS genes in tomato were analyzed based on a real-time quantitative PCR assay and an analysis of a public expression dataset. SAMS genes of monocots were more conserved according to the results of a phylogenetic analysis and the prediction of phosphorylation and glycosylation patterns. SAMS genes showed differential expression in response to abiotic stresses and exogenous hormone treatments. Solyc01g101060 was especially expressed in fruit and root tissues, while Solyc09g008280 was expressed in leaves. Additionally, our results revealed that exogenous BR and ABA treatments strongly reduced the expression of tomato SAMS genes. Our research provides new insights and clues about the role of SAMS genes. In particular, these results can inform future functional analyses aimed at revealing the molecular mechanisms underlying the functions of SAMS genes in plants.

Keywords: genome analysis; post translation modifications; miRNAs target site; hormones; abiotic stress

1. Introduction

S-Adenosyl-L-methionine (SAM) is a key molecule in eukaryotic cells that participates in several important biological reactions [1–3]. SAM is catalyzed from methionine and adenosine triphosphate (ATP) by the enzyme S-adenosylmethionine synthetase (SAMS) [3]. SAM is involved in different pathways, such as ethylene (in plants), nicotianamine and polyamine biosynthesis pathways; transmethylation and transsulfuration pathways, and the methionine metabolism pathway [4,5] (Figure 1). In addition, SAM participates in lignin biosynthesis and responses to environmental stresses, and it has essential roles in several cellular processes [6,7]. SAM is widely known as a methyl group donor, with many proteins, nucleic acids, phospholipids, and small molecules being methylated mainly by SAM [8]. SAM, as a sulfonium salt, has a sulfur atom in its structure that is involved in transferring the methyl group to nucleophilic atoms such as carbon atom (in C5-cytosine of DNA strands), nitrogen atom (in amino group of glycine), sulfur atom (in S-methylation reaction of thiopurines), oxygen atom (in O-methylation reaction of catecholamine) and arsenic atom [9,10].

Furthermore, aminopropyl groups involved in polyamine and ethylene biosynthesis and methylene groups involved in cyclopropyl fatty acid biosynthesis use SAM as a methyl donor source [3].

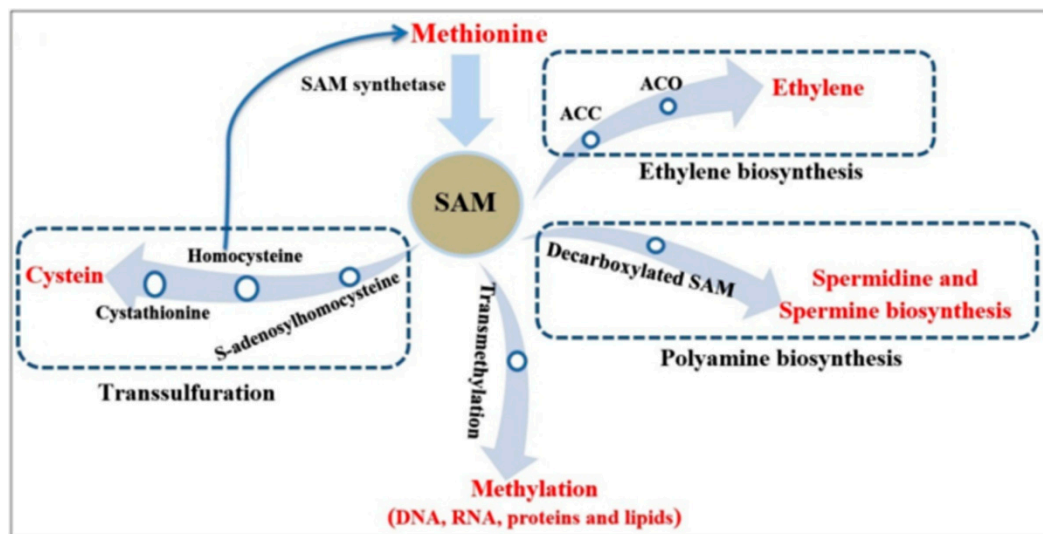


Figure 1. Metabolic and biosynthesis pathways involving SAM.

In the transsulfuration pathway, SAM enzyme participates in the conversion of homocysteine to cysteine as a precursor of cellular antioxidants such as glutathione [1]. After methylation, SAM is converted to S-adenosylhomocysteine (SAH), which is a vigorous inhibitor of methylation reactions. S-adenosylhomocysteine hydrolase enzyme converts SAH to homocysteine and adenosyl [11]. Recent studies have shown that several human diseases, such as stroke, dementia, osteoporosis, Alzheimer disease and coronary artery disease, are correlated with plasma total homocysteine [11–13]. Furthermore, SAM is a substrate for polyamine and ethylene biosynthesis. Polyamines are important hormones in eukaryote organisms and regulate cell growth during several activities, including stress responses, pollen and flower development and protection of photosystem II [1,5,14]. In polyamine biosynthesis, SAM is converted to S-adenosylmethioninamine enzyme (also known as decarboxylated SAM) by S-adenosylmethionine decarboxylase (SAMDC) [5]. S-adenosylmethioninamine, as an aminopropyl donor, is used in the biosynthesis of polyamines, such as spermine and spermidine from putrescine (Figure 1) [5]. In addition, SAM participates in the synthesis of 1-aminocyclopropane-1-carboxylic acid (ACC) by ACC synthase (ACS); ACC, as a precursor, is converted to ethylene by ACC oxidase (ACO) [15,16]. Previous studies show that genes involved in the SAM cycle (Figure 1) play important roles in regulating cell growth and stress responses. For instance, the downregulation of SAMDC genes reduces pollen viability, plant length and abiotic stress tolerance in transgenic rice [17]. In addition, overexpression of SAMDC increases drought tolerance in *Arabidopsis* [18], sodium chloride-stress tolerance in rice [19], and biotic and abiotic stress tolerance in tomato [20].

SAM synthetase (SAMS) enzyme, also known as methionine adenosyltransferase (MAT), catalyzes SAM from methionine. Espartero et al. [21] found that SAMS genes of tomato have differential expression in response to salt stress. In addition, Li et al. [22] observed that overexpression of the SAM synthetase gene of *Lycoris radiata* in *E. coli* can promote plant tolerance to salt stress. Furthermore, Mao et al. [23] found that a plasma membrane receptor-like kinase, FERONIA (FER), negatively regulates the synthesis of SAM by SAMS in *Arabidopsis* and that ethylene and SAM content are increased in a *fer* mutant. Interestingly, Erb et al. [24] detected an unexpected link between SAM metabolism and RubisCO-like protein in the central carbon metabolism of *Rhodospirillum rubrum*.

The above-mentioned observations indicate that the SAMS gene family plays critical roles in the metabolism of plant species and is involved in regulating cell growth and gene expression.

Several studies have examined the roles of SAMS genes in human diseases, but comparative studies of the structure, physicochemical properties, and expression of SAMS gene family in plants are lacking. In this study, we conducted a comparative investigation of SAMS genes in dicots (*Arabidopsis*, tomato, eggplant, sunflower, *Medicago truncatula*, and soybean) and monocots (rice, barley, *Triticum urartu* and sorghum), with focus on their structure, physicochemical characteristics and post-transcriptional and post-translational modifications (miRNA targets, phosphorylation, and glycosylation). Additionally, using RNA-seq data, we studied the gene expression of SAMS genes under different treatments in tomato. Furthermore, the gene expression patterns of tomato-SAMS genes were investigated under abiotic stresses (salt, cold, heat, and water stress) and hormone treatments (brassinosteroid, salicylic acid, auxin, and abscisic acid) using real-time quantitative PCR (RT-qPCR) assay. This study yields important information about SAMS genes that can inform future studies of the functions of SAMS genes.

2. Results

2.1. Physicochemical Properties of SAMS Genes

The physicochemical properties of the SAMS genes are shown in Table 1. The table lists gene ID, amino acid sequence length, molecular weight, isoelectric point, instability index, aliphatic index, GRAVY value, and subcellular localization. In our study, the number of SAMS genes in the selected plant species varied from 3 to 9, and the highest copy number was observed in soybean. The length of the amino acid sequence ranged from 238 to 479, with HanXRQChr01g0027791 (sunflower SAMS) being the smallest protein and EMS52834.1 (*T. urartu* SAMS) being the largest protein. The molecular weight (MW) of the studied SAMS proteins ranged from 26.22 to 52.80 KDa. The isoelectric point (pI) varied from 5.22 to 9.13; LOC_Os01g18860 (rice SAMS) was predicted to be an acidophilic protein, while HanXRQChr01g0027791 was predicted to be an alkaline protein. According to the protein instability index values, all studied SAMS proteins were stable. The aliphatic index, a measure of thermostability, varied from 79.87 to 92.52. The predicted GRAVY value of the studied SAMS proteins ranged from -0.353 to -0.153 , and most of the SAMS genes showed negative values, indicating hydrophilic properties. The prediction of subcellular localization showed that the most SAMS proteins were localized in the cytoplasm. However, most SAMS proteins of sunflowers were predicted to localize in the chloroplast (Table 1).

2.2. Phylogenetic and Conserved Motif Analyses of the SAMS Gene Family

The evolutionary relationships of the SAMS genes were analyzed by the multiple alignment of the amino acid sequences from *Arabidopsis*, tomato, eggplant, sunflower, barley, rice, sorghum, *Medicago truncatula*, *Triticum urartu* and soybean using the neighbor-joining method (Figure 2). The phylogenetic analysis clustered the SAMS genes of the selected plant species into five major groups. All SAMS genes of monocots were located in the first group, while those of dicots were clustered into four different groups. In addition, the SAMS genes of group V showed more variability than the SAMS genes of the other groups (Figure 2). According to the phylogenetic analysis, the SAMS genes of soybean, *M. truncatula*, and *Arabidopsis* were more similar to each other than to the other SAMS genes. Moreover, we evaluated the conserved motifs according to the phylogenetic analysis to gain insight into the structural features of SAMS members in selected plants. The conserved motifs were predicted using the MEME server; 10 conserved motifs in the SAMS proteins were predicted (Figure 3). All members of the SAMS gene family contain motifs 1, 2, 3 and 8 (Figure 3). Determining the functions of these conserved motifs may provide insight into the functions and interactions of SAMS genes.

Table 1. The properties of SAMS genes in the studied plants.

| Organism | Locus ID | Length (aa) | MW (KDa) | pI | Instability Index | Aliphatic Index | GRAVY | Subcellular Localization |
|---------------------|-------------------------|-------------|----------|--------|-------------------|-----------------|-----------|--------------------------|
| Arabidopsis | AT2G36880 | 390 | 42.497 | 5.76 | stable | 83.74 | −0.236 | Cytoplasm |
| | AT4G01850 | 393 | 43.255 | 5.67 | stable | 79.34 | −0.353 | Cytoplasm |
| | AT3G17390 | 393 | 42.796 | 5.51 | stable | 85.04 | −0.255 | Cytoplasm |
| | AT1G02500 | 393 | 43.158 | 5.51 | stable | 80.33 | −0.306 | Cytoplasm |
| Tomato | Solyc01g101060.3 | 393 | 43.301 | 5.51 | stable | 82.80 | −0.335 | Cytoplasm |
| | Solyc09g008280.2 | 390 | 42.652 | 5.76 | stable | 82.95 | −0.283 | Cytoplasm |
| | Solyc10g083970.1 | 390 | 42.660 | 6.12 | stable | 80.97 | −0.313 | Cytoplasm |
| Eggplant | Solyc12g099000.2 | 393 | 43.082 | 5.41 | stable | 84.05 | −0.313 | Cytoplasm |
| | Sme2.5_00004.1_g00028.1 | 390 | 42.624 | 5.76 | stable | 81.97 | −0.290 | Cytoplasm |
| | Sme2.5_00187.1_g00013.1 | 393 | 43.122 | 5.68 | stable | 84.30 | −0.307 | Cytoplasm |
| | Sme2.5_07249.1_g00002.1 | 394 | 43.367 | 5.49 | stable | 82.34 | −0.331 | Chloroplast |
| Sunflower | Sme2.5_07301.1_g00003.1 | 390 | 42.627 | 6.08 | stable | 81.23 | −0.305 | Cytoplasm |
| | HanXRQChr01g0027791 | 238 | 26.223 | 9.13 | stable | 92.52 | −0.153 | Cytoplasm |
| | HanXRQChr01g0027801 | 390 | 42.969 | 5.97 | stable | 81.97 | −0.346 | Cytoplasm |
| | HanXRQChr02g0051721 | 457 | 49.894 | 5.93 | stable | 84.03 | −0.227 | Chloroplast |
| | HanXRQChr05g0148381 | 455 | 49.847 | 5.42 | stable | 83.76 | −0.257 | Chloroplast |
| | HanXRQChr07g0194741 | 453 | 49.887 | 5.97 | stable | 83.05 | −0.237 | Chloroplast |
| | HanXRQChr13g0400841 | 437 | 48.132 | 6.22 | stable | 83.62 | −0.291 | Chloroplast |
| Triticum urartu | HanXRQChr14g0454811 | 341 | 37.276 | 6.42 | stable | 84.34 | −0.297 | Cytoplasm |
| | XP_020178978.1 | 394 | 42.765 | 5.52 | stable | 85.86 | −0.203 | Cytoplasm |
| | EMS55466.1 | 394 | 42.788 | 5.61 | stable | 84.39 | −0.212 | Cytoplasm |
| Barley | EMS52834.1 | 479 | 52.800 | 6.51 | stable | 81.98 | −0.290 | Chloroplast |
| | HORVU6Hr1G034650 | 396 | 43.158 | 5.33 | stable | 81.72 | −0.253 | Cytoplasm |
| | HORVU6Hr1G063490 | 394 | 42.766 | 5.52 | stable | 85.86 | −0.203 | Chloroplast |
| | HORVU6Hr1G063540 | 394 | 42.814 | 5.49 | stable | 83.40 | −0.219 | Cytoplasm |
| Rice | HORVU6Hr1G063560 | 394 | 42.828 | 5.58 | stable | 83.40 | −0.220 | Cytoplasm |
| | LOC_Os01g222010 | 394 | 42.901 | 5.68 | stable | 81.14 | −0.264 | Cytoplasm |
| | LOC_Os01g18860 | 396 | 43.310 | 5.22 | stable | 82.70 | −0.274 | Cytoplasm |
| Sorghum | LOC_Os05g04510 | 396 | 43.220 | 5.74 | stable | 82.45 | −0.289 | Cytoplasm |
| | Sobic.003G140000 | 396 | 43.257 | 5.32 | stable | 83.69 | −0.284 | Cytoplasm |
| | Sobic.003G151600 | 394 | 42.785 | 5.50 | stable | 82.13 | −0.237 | Cytoplasm |
| | Sobic.009G033600 | 396 | 42.976 | 5.57 | stable | 83.21 | −0.260 | Cytoplasm |
| Medicago truncatula | Medtr1g063060 | 408 | 44.904 | 6.24 | stable | 81.67 | −0.294 | Cytoplasm |
| | Medtr2g046710 | 396 | 43.174 | 5.77 | stable | 83.43 | −0.287 | Cytoplasm |
| | Medtr4g123810 | 393 | 42.916 | 5.67 | stable | 85.29 | −0.254 | Cytoplasm |
| | Medtr7g102120 | 390 | 42.654 | 6.36 | stable | 82.46 | −0.300 | Cytoplasm |
| | Medtr7g110310 | 394 | 43.279 | 5.59 | stable | 80.86 | −0.327 | Cytoplasm |
| Soybean | Glyma.07G233800 | 392 | 43.055 | 5.65 | stable | 82.53 | −0.330 | Cytoplasm |
| | Glyma.10G144300 | 389 | 42.620 | 5.41 | stable | 85.42 | −0.259 | Cytoplasm |
| | Glyma.17G039000 | 392 | 42.981 | 5.43 | stable | 83.52 | −0.328 | Cytoplasm |
| | Glyma.03G184000 | 390 | 42.727 | 6.13 | stable | 81.46 | −0.298 | Cytoplasm |
| | Glyma.03G223000 | 394 | 43.224 | 5.57 | stable | 80.13 | −0.337 | Cytoplasm |
| | Glyma.19G220200 | 394 | 43.250 | 5.57 | stable | 79.87 | −0.345 | Cytoplasm |
| | Glyma.10G054500 | 390 | 42.608 | 5.86 | stable | 82.46 | −0.283 | Cytoplasm |
| | Glyma.13G141600 | 390 | 42.586 | 5.82 | stable | 82.46 | −0.276 | Cytoplasm |
| Glyma.15G190500 | 395 | 43.053 | 5.50 | stable | 82.89 | −0.304 | Cytoplasm | |

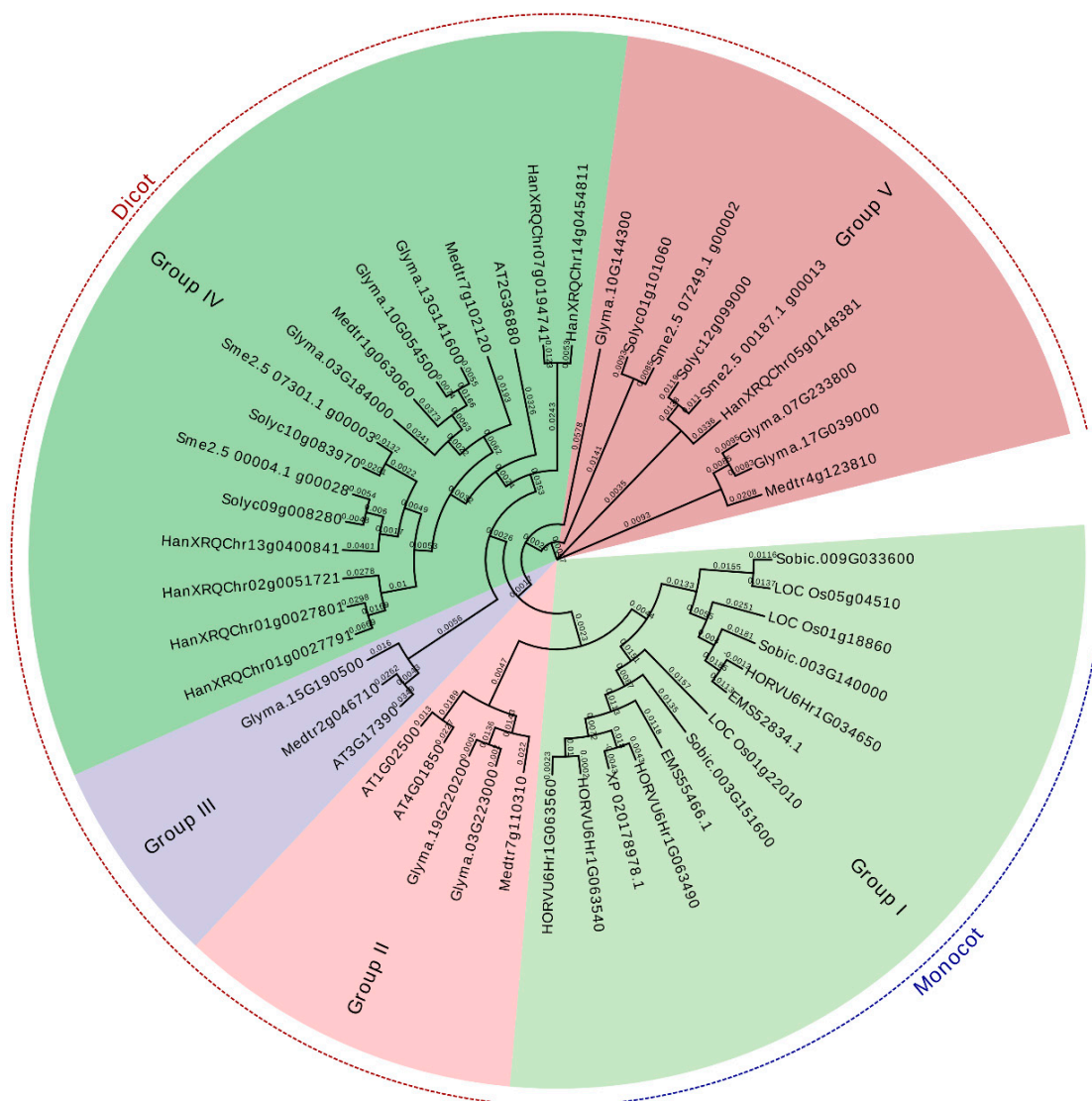


Figure 2. Phylogenetic tree of SAMS gene-based amino acid sequences using the neighbor-joining method of Clustal Omega.

2.3. Prediction of Phosphorylation and Glycosylation Sites

In this study, the phosphorylation and glycosylation sites were predicted to provide insight into the post-translation modifications of SAMS proteins. The potential phosphorylation sites of SAMS proteins were predicted using the NetPhos 3.1 server (Figure 4). The number of predicted phosphorylation sites ranged from 19 in HanXRQChr01g0027791 to 47 in HanXRQchr07g0194741 (sunflower SAMS). The most studied SAMS proteins had 30 to 40 predicted phosphorylation sites, and most of the variation was observed among the SAMS proteins of sunflower. Among the studied SAMS proteins, three sunflower SAMS proteins (HanXRQChr07g0194741, HanXRQChr02g0051721 and HanXRQChr05g0148381) were identified as serine-rich proteins (Figure 4). The amino acid sequences of SAMS proteins were analyzed using the NetNGlyc 1.0 server to predict N-glycosylation sites. The prediction results revealed that most SAMS proteins were glycosylated at two conserved sites (Figure 5). The amino acid 235/236 was predicted to be a conserved glycosylation site in all studied SAMS proteins of monocots.

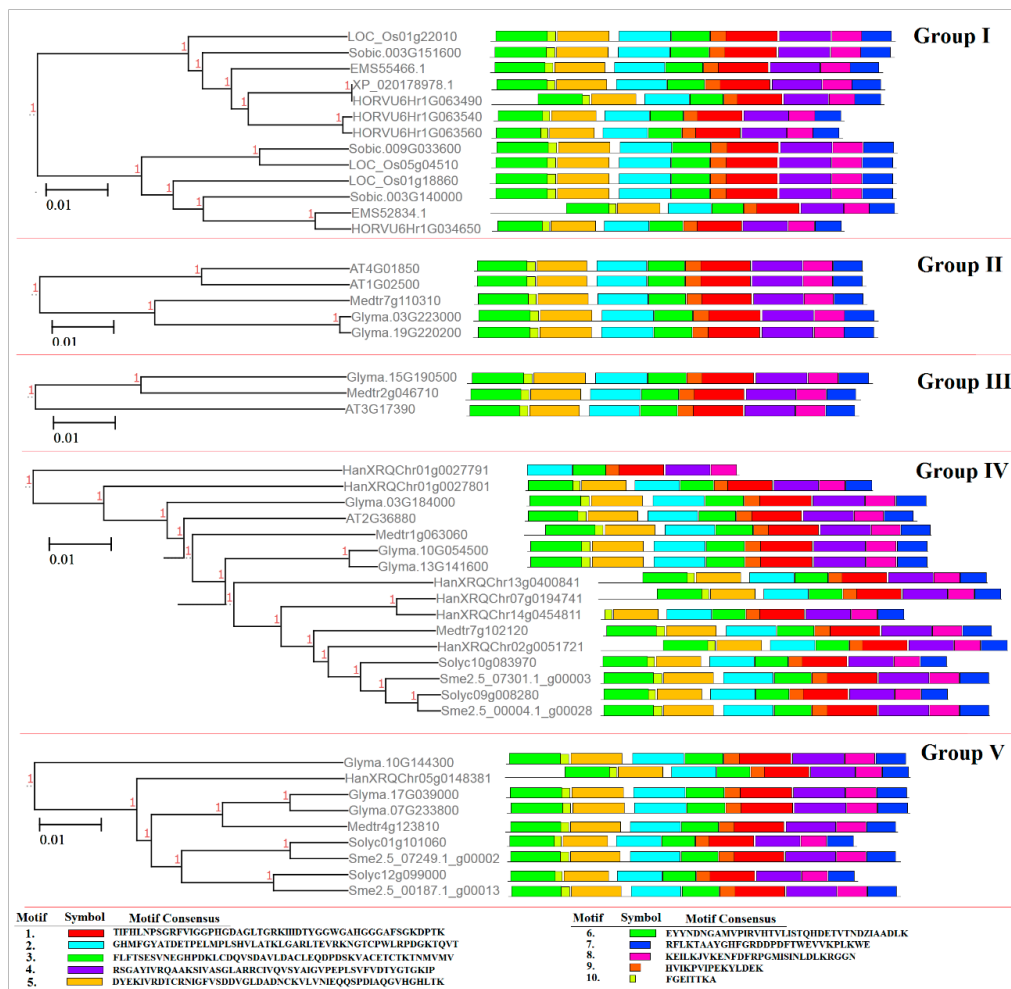


Figure 3. Conserved motif distribution of SAMS proteins in the studied plant species predicted using the MEME v4.12.0 server.

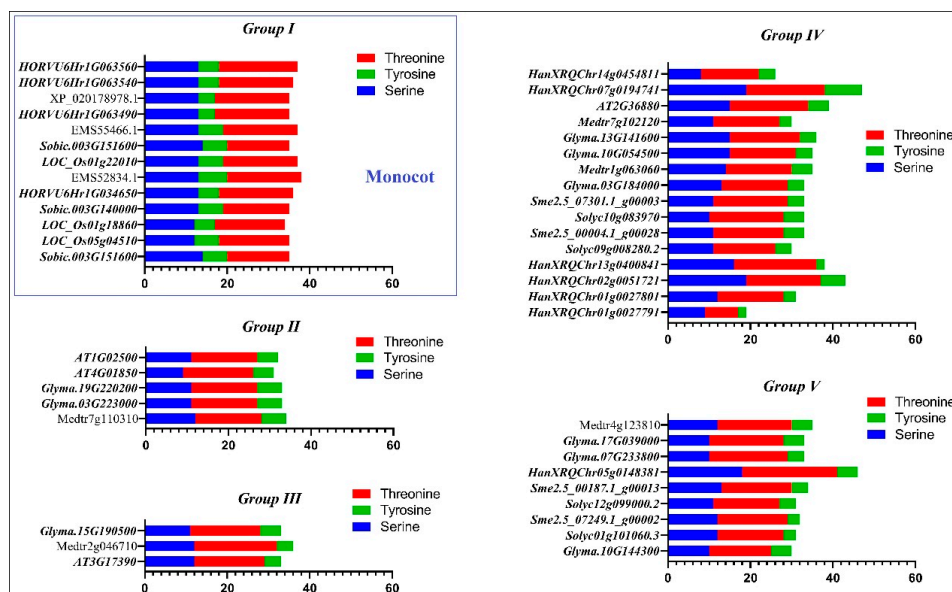


Figure 4. Predicted phosphorylation sites of SAMS proteins in different plant species determined using the NetPhos 3.1 server.

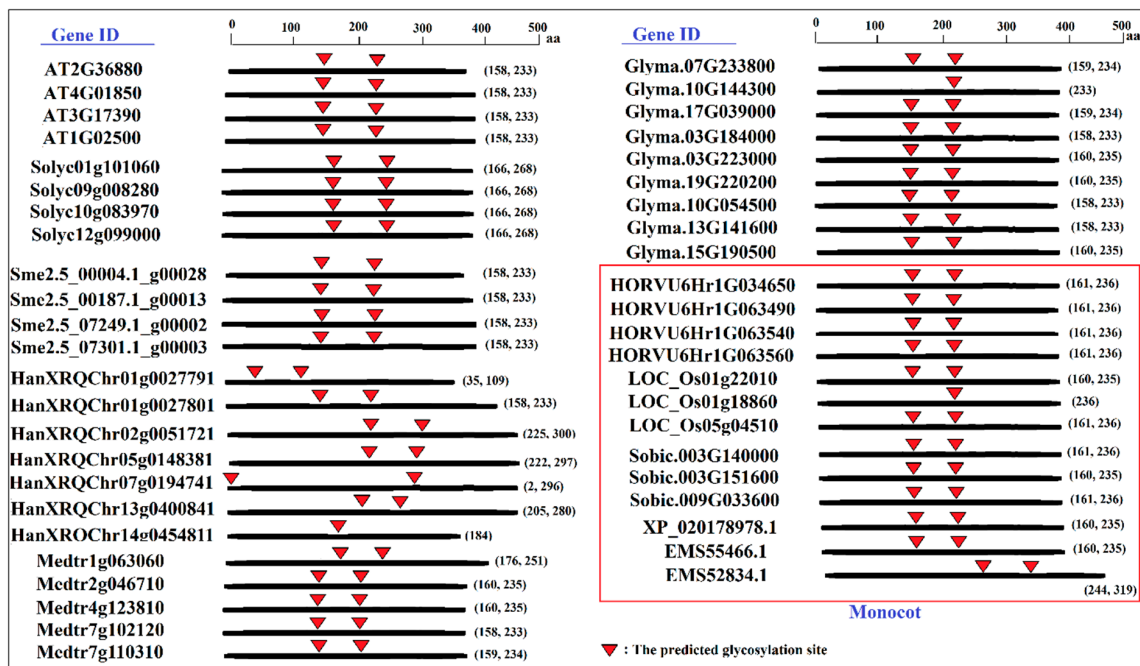


Figure 5. Predicted glycosylation sites of SAMS proteins in different plant species determined using the NetNGlyc 1.0 server.

2.4. Prediction of MicroRNA Target Sites

MicroRNAs are noncoding RNAs that play critical roles in many biological processes. The transcript sequences of SAMS genes were screened to predict the target sites of plant microRNAs using the psRNA target server. The prediction of miRNA-target sites revealed that transcripts of SAMS genes were targeted by plant miRNAs at an expectation level ≤ 2.5 (Figure 6). The binding sites of other miRNAs with lower complementarity (expectation level < 4) were also predicted, as shown in Table S2. The binding sites of gma-miR1520 and mtr-miR5275 were observed in transcript sequences of two soybean SAMS genes, Glyma.19G220200 and Glyma.10G054500. Furthermore, the pre-mRNA of LOC_Os01g18860, a rice-SAMS gene, was targeted by osa-miR5528. In addition, the binding site of osa-miR415 was observed in transcript sequences of the Medtr7g110310 gene, and a barley SAMS gene (HORVU6Hr1G0634490) was predicted to be targeted by hvu-miR6197. According to our results, SAMS genes can be regulated by different miRNAs and that members of this complex (SAMS-miRNAs) can affect downstream pathways related to SAM.

2.5. Transcriptional Profiling of SAMS Genes in Tomato

To reveal the expression patterns of SAMS genes in different tissues and conditions, the available RNA-seq data of tomato species were analyzed. A heat map of tomato SAMS genes is shown in Figure 7. The expression patterns revealed that tomato SAMS genes were differentially expressed among tissues. For instance, Soly01g101060 gene was especially expressed in fruit tissues (Figure 7a) and was strongly upregulated in the mature green fruit of tomato (at 39 days post anthesis). Among the tomato SAMS genes, the Soly01g101060 gene showed the highest expression in root tissues, and it was downregulated in root tissues when the temperature was altered from 23 °C to 15 °C (Figure 7b). Furthermore, Soly09g008280 showed higher expression in leaves than in other tissues (Figure 7c,d), while Soly12g099000 showed weak expression in all analyzed samples. According to the RNA-seq results, Soly09g008280 was more upregulated than were other genes under biotic stresses, such as treatment with *P. syringae* pv. Tomato DC3000 and nightly red light treatment (Figure 7c).

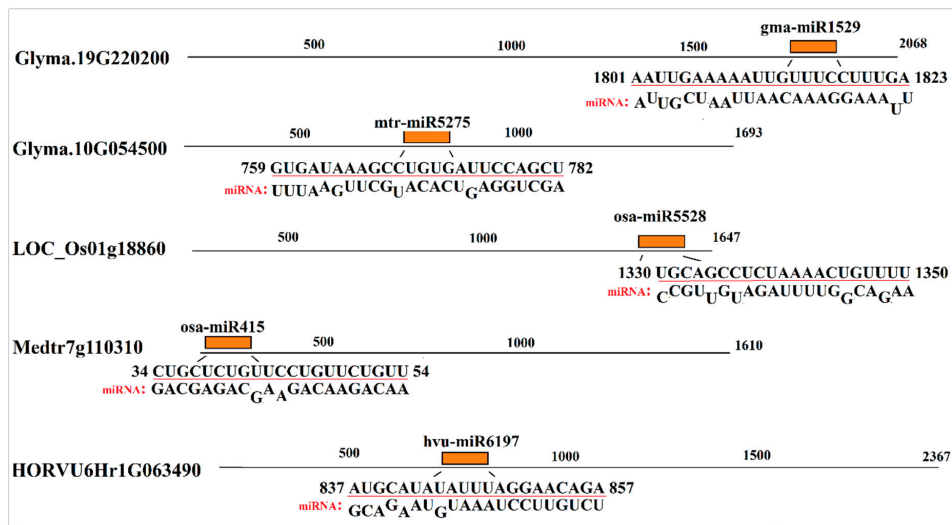


Figure 6. Predicted sites of microRNA targets in transcript sequences of the studied SAMS genes identified using the psRNATarget server.

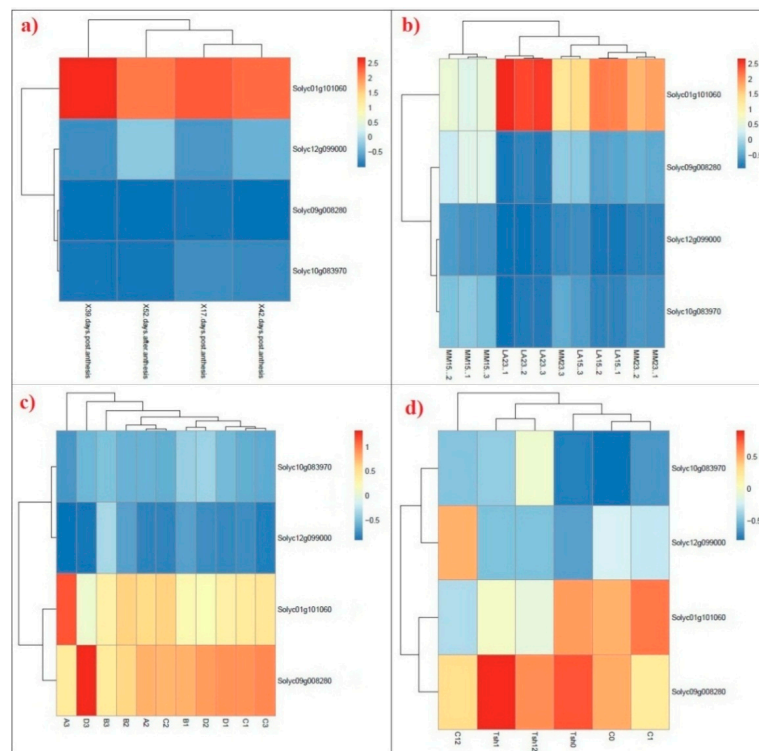


Figure 7. Heat map of the expression profiles of tomato SAMS genes under different stresses. (a) transcription profile of SAMS genes at developmental stages of tomato fruit obtained from RNA-seq dataset with accession ID: E-MTAB-4818 (X17, 39, 42, and 59 denote 17, 39, 42, and 52 days post-anthesis, respectively); (b) transcription profile of SAMS genes in tomato roots under low temperature stress obtained from RNA-seq dataset with accession ID: E-MTAB-4855 (LA23: *S. habrochaites* LA1777 at 23 °C; LA15: *S. habrochaites* LA1777 at 15 °C; MM23: *S. lycopersicum* Moneymaker at 23 °C; LA15: *S. lycopersicum* Moneymaker at 15 °C); (c) transcription profile of SAMS genes in tomato shoot under biotic stress [25], (A: control; B: treatment with *Pseudomonas syringae* pv. Tomato DC3000; C: nightly red light treatment; D: treatment with *P. syringae* pv. Tomato DC3000+ nightly red light treatment); (d) transcription profile of SAMS genes in tomato shoot under cold stress [26], (C0, C1 and C12: *S. lycopersicum* at 0, 1, and 12 h at 4 °C, respectively; Tsh0, Tsh1, and Tsh12: *S. habrochaites* at 0, 1, and 12 h at 4 °C, respectively).

2.6. Expression Patterns of Tomato SAMS Genes Determined via qRT-PCR

The expression patterns of members of a gene family can reveal aspects of their functions under different biological conditions. To elucidate the potential biological roles of tomato SAMS genes, their expression patterns were studied under four different abiotic stresses (salt, cold, heat, and water) and various exogenous hormone treatments (brassinosteroid (BR), salicylic acid (SA), auxin, abscisic acid (ABA)). qRT-PCR demonstrated that the SAMS genes were differentially expressed between each abiotic stress and control conditions (Figure 8). *Solyc12g099000* was downregulated under all abiotic stresses, especially under water stress. *Solyc01g101060* and *Solyc09g008280* expression was correlated with heat and water stress, which was downregulated under heat stress and strongly downregulated in response to water stress. In this study, the relative expression of *Solyc10g083970* was significantly increased in response to water stress, in contrast to that of the other studied tomato SAMS genes. Moreover, *Solyc01g101060* and *Solyc09g008280* showed similar expression patterns in response to abiotic stresses. In addition, the expression of tomato SAMS genes was induced in response to exogenous hormonal treatments (Figure 8). All tomato SAMS genes were strongly downregulated in response to exogenous BR application. Furthermore, a significant decrease was observed in the expression of *Solyc12g099000*, *Solyc09g008280*, and *Solyc10g083970* under ABA treatment. In addition, exogenous SA treatment did not affect *Solyc12g099000* and *Solyc01g101060* expression but caused downregulation of *Solyc09g008280* and *Solyc10g083970*. Our results revealed that exogenous hormonal application reduced the expression of tomato SAMS genes.

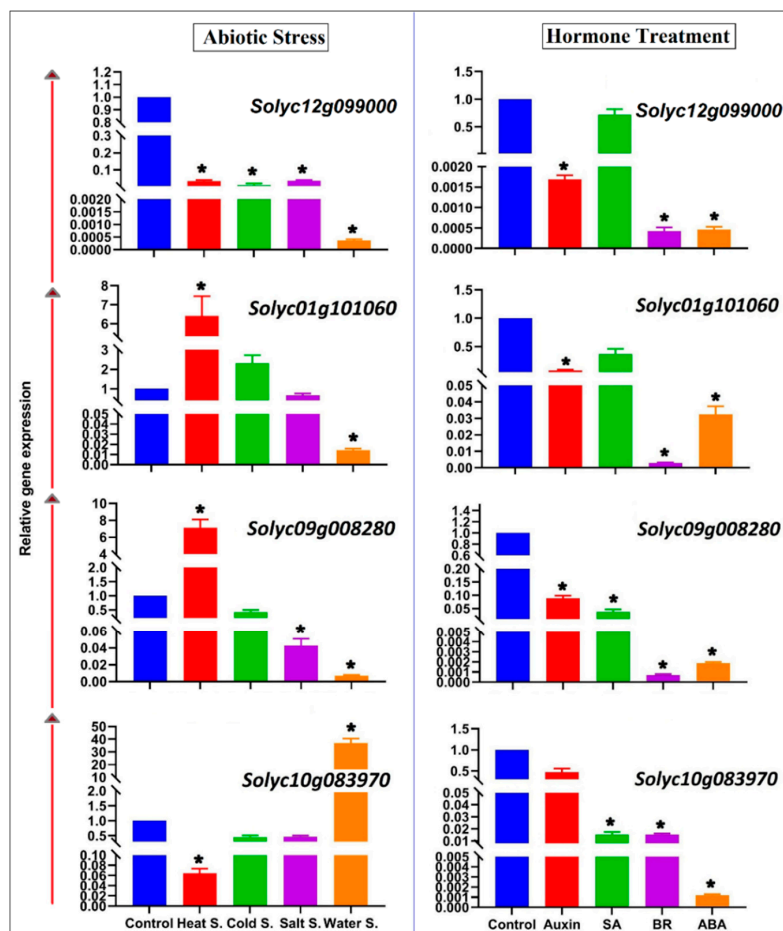


Figure 8. Expression patterns of SAMS genes under abiotic stress and hormone treatments. An asterisk above a bar indicates a significant difference between the experimental treatments and control treatment (according to Student's *t*-test).

3. Discussion

SAM is a key molecule involved in multiple cellular pathways, such as pathways related to ethylene and polyamine biosynthesis, methionine metabolism, and transmethylation and transsulfuration [4,5]. In the current study, SAM synthetase genes in different plant species were analyzed by an extensive use of bioinformatics tools. The SAMS genes in the selected plant species exhibited variation in GRAVY value, protein length, aliphatic index, isoelectric point, molecular weight, and instability index (Table 1). According to the instability index values, all of the studied SAMS proteins were stable. The instability index of a protein indicates the enzyme's stability over reaction time [27]. In addition, the SAMS proteins showed high aliphatic index values, which confers high thermal stability and long half-lives to proteins [28]. Protein stability refers to the ability of a protein to retain function and structure in a specific condition. SAM is involved in several different pathways, and high stability preserves SAM structure in various cellular reactions. The predicted values of GRAVY, a solubility index [29], showed that the SAMS proteins of monocots, such as rice, sorghum, and barley, were less hydrophilic than the those of the studied dicot plants. In addition, cytosol and chloroplast were predicted as the subcellular localizations of SAMS proteins. SAM is localized in cytosol and can be transferred into chloroplast by specific carriers [30]. Methionine synthesis and S-adenosylmethionine (SAM) metabolism in plants can occur in chloroplast [30]. According to physicochemical results, it seems that SAMS proteins are thermostable proteins and can be employed in high-temperature reactions.

According to the phylogenetic analysis, the motifs of group I were more conserved, indicating that dicot SAMS genes are probably derived from monocot SAMS genes. In particular, four conserved motifs found in all studied SAMS proteins are associated to general functions of these proteins. Besides, other conserved motifs observed in the same group reveal new insights on group-specific functions for SAMS proteins. In addition, the post-translational modifications of SAMS proteins were predicted based on phosphorylation and glycosylation sites. Phosphorylation and glycosylation processes are known as post-translational modifications in eukaryote organisms that play key roles in protein functions [27]. Phosphorylation plays key roles in signal transduction, protein-protein interactions and plant metabolism by modifying protein activities [31–33]. In the current study, the number of prediction phosphorylation sites ranged from 19 to 47, and three sunflower SAMS proteins (HanXRQChr07g0194741, HanXRQChr02g0051721 and HanXRQChr05g0148381) were identified as serine-rich proteins. Serine-rich proteins are highly phosphorylated, and most serine-rich proteins have pleiotropic effects on phenotypes and regulate various processes [34]. Phosphorylation can regulate several processes that affect features such as the stability and subcellular localization of proteins [27]. In this study, variation in the subcellular localization of serine rich-SAMS proteins was observed. Glycosylation can alter the molecular weight and stability of a protein [27,35]. Most proteins involved in the secretory pathway are extensively glycosylated in the endoplasmic reticulum [36]. According to glycosylation prediction results, most of the studied SAMS proteins were glycosylated in two conserved sites. These locations can be investigated in further studies related to functional genomics. The prediction results regarding miRNA targeting sites in transcript sequences of SAMS genes revealed that SAMS transcripts can be targeted by putative microRNAs. MicroRNAs or miRNAs compose a group of short, noncoding RNAs that have critical roles in many biological processes, including cell proliferation, development, organogenesis, and stress responses [37]. MiRNAs can regulate gene expression after transcription in collaboration with RNA-induced silencing complexes (RISCs) [38]. In this study, the target sites of gma-miR1520 and mtr-miR5275 in transcript sequences of soybean SAMS genes were predicted. Gma-miR1520 is involved in the responses to soybean cyst nematode infection and salt stress [39,40], while mtr-miR5275 is associated with arbuscular mycorrhizal symbiosis [41]. In addition, the target sites of osa-miR5528, osa-miR415, and hvu-miR6197 in transcript sequences of SAMS genes were observed. Osa-miR5528 has been identified as being involved in rice inflorescence at heading stage and in the response to drought stress [42], and osa-miR415 is involved in the response to rice stripe virus [43]. Furthermore, hvu-miR6197 is associated with the response to excess boron in barley [44]. MicroRNAs can alter the expression of target pre-mRNAs that are also

regulated by several factors, such as biotic and abiotic stress. According to our results, SAMS genes can be regulated by different miRNAs in this complex (SAMS-miRNAs) to affect downstream pathways related to SAM.

The expression patterns of a gene family can reveal aspects of their functions under different biological conditions. To gain insight into the expression patterns of Arabidopsis SAMS genes, public microarray datasets [45] for different organs and stages of development and various abiotic and biotic stresses were analyzed (Figure 9). The results indicated that the expression patterns of SAMS genes varied among organs in Arabidopsis and tomato. Furthermore, SAMS genes showed differential expression from control expression in response to biotic and abiotic stresses. For example, *SAMS3* and *SAMS4* of Arabidopsis were upregulated under biotic stress and BR treatment and downregulated in response to abiotic stresses such as salt, heat and temperature stress and ABA application. The findings confirmed that BR can enhance pathogen resistance [46]. ABA is known as a hormone responsive to abiotic stresses such as drought, heat, low temperature, radiation and salt stress [47]. Besides, the transcript sequence of Arabidopsis-SAM3 is targeted by miR5021 (Table S2). Previous studies reported that miR5021 is involved in several pathways. For instance, miR5021 in *Mentha* spp. regulates genes that encode for enzymes involved in the essential oil biosynthesis [48]. In *Arabidopsis*, miR5021 negatively regulated genes involved in the abscisic acid signaling pathway and cell growth and indirectly linked with leaf senescence [49].

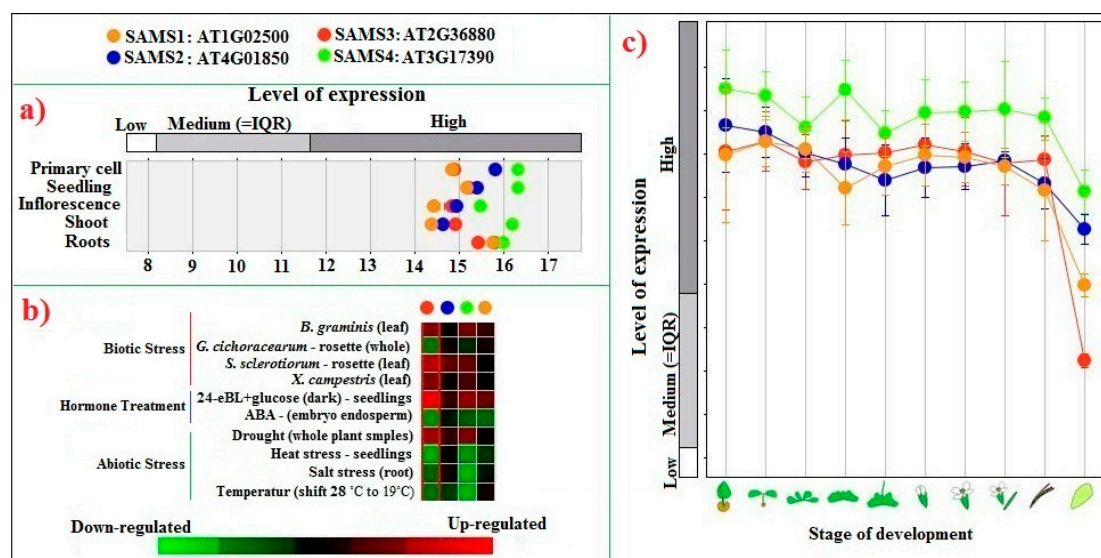


Figure 9. Expression levels of Arabidopsis SAMS genes in various tissues and organs (a) under different biotic and abiotic stresses and hormone treatments; (b) and at different development stages; (c) The data were obtained from Affymetrix Arabidopsis ATH1 genome array (10,615 samples) using Genevestigator [45].

According to the expression patterns of tomato SAMS genes, the *Solyc01g101060* gene was especially expressed in fruit and root tissues, while *Solyc09g008280* gene was expressed primarily in leaves (Figure 7). These results revealed that tomato SAMS genes have tissue-specific expression patterns. Tissue-specific expression can provide insight into the different functions of target genes in different organs [50,51]. The qRT-PCR results revealed that *Solyc01g101060* and *Solyc09g008280* were downregulated under heat stress and water stress and that the expression of the *Solyc10g083970* gene was downregulated under all abiotic stresses and hormone treatments (Figure 8). All studied tomato SAMS genes showed downregulation in response to salt stress. Wang et al. [52] similarly found that soybean SAMS genes are downregulated in root tissues in response to flooding and drought stresses. However, Sánchez-Aguayo et al. [53] reported that the expression of SAMS genes is increased in roots of tomato under salinity stress, and they observed a positive correlation between SAM activity

and lignin deposition in the vascular tissues in response to salt stress. Similarly, Espartero et al. [21] found that the mRNA level of *SAMS1* is increased in response to NaCl stress in leaf tissue of tomato and that their transcript patterns can be maintained for at least 3 days. In addition, SAM enzyme is involved in glycine betaines biosynthesis as a key osmoprotectant under salt stress [54]. In this study, tomato SAMS genes showed differential expression in response to different stresses. Tomato SAMS genes were investigated under hormone treatments, and their expression patterns were found to be downregulated in response to exogenous hormone treatments. In particular, BR strongly decreased the expression pattern of SAMS genes (Figure 8). Phytohormones such as BR and auxin can reduce ethylene biosynthesis in Arabidopsis by interacting with SAM synthases, and ethylene biosynthesis has been shown to decrease in double mutant lines of *SAMS1* and *SAMS2* (*mat1* and *mat2*) [23]. Both auxin and BR may negatively control the SAMS genes (*SAMS1* and *SAMS2* of Arabidopsis) from FERONIA (FER) as a receptor-like kinase of plasma membrane [23]. It is also known that exogenous application of BR decreases the free ACC and ethylene content in root and shoot tissue but maintains the polyamines level in lettuce plants under salt stress [55]. In the present study, the expression of *Solyc12g099000*, *Solyc09g008280*, and *Solyc10g083970* was significantly decreased under ABA treatment. SAMS genes have multiple biological roles, including participation in methionine metabolic pathways [4], and they have crucial roles in ethylene and polyamine biosynthesis and plant cell signaling [52,56]. However, ethylene and polyamine have antagonistic effects to each other. Polyamines can reduce the ethylene biosynthesis by controlling expression of ACC synthase (ACS) and ethylene can inhibit the activity of enzymes involved in polyamine biosynthesis such as SAMDC [57]. The enzyme ACS that catalyzes ACC from SAM (for details see Figure 1) is introduced as a regulatory crosstalk point between ethylene biosynthesis and polyamine pathway [15]. Moreover, this enzyme is encoded by multi ACS genes that have differential expression in response to distinct inducers affecting the conversion of SAM to ACC in ethylene biosynthesis [15]. The overexpression of SAMS in tobacco was found to induce the expression levels of SAMDC under cold stress while ACS and ACO are not affected [58,59]. In alfalfa, the expression of SAM1 gene was found associated with polyamines in response to cold stress [58], suggesting a positive correlation between SAM activity and SAMDC under abiotic stress. Our results are consistent with previous findings as this study reveals that SAMS genes are involved in hormone signaling and that ABA and BR can negatively regulate downstream pathways related to SAMS genes.

4. Materials and Methods

4.1. Identification and Sequence Analysis of SAMS Genes

Protein sequences of SAMS genes in *Arabidopsis thaliana* were obtained from the Arabidopsis Information Resource (TAIR10) database (<ftp://ftp.arabidopsis.org>). The protein sequences of Arabidopsis-SAMS genes were used as queries in a BLASTp analysis against the proteomes of tomato, eggplant, sunflower, barley, rice, *Triticum urartu*, sorghum, *Medicago truncatula* and soybean to identify SAMS proteins. To assess the presence of the protein domain S-adenosylmethionine synthetase, all predicted-SAMS proteins were analyzed by Conserved Domain Database (<https://www.ncbi.nlm.nih.gov/Structure/cdd/cdd.shtml>). The biochemical properties of selected proteins, including protein length, molecular weight (MW), isoelectric point (pI), instability index, aliphatic index and the grand average of hydropathy (GRAVY), were predicted by ExPASy ProtParam [60] (<https://web.expasy.org/protparam/>). In addition, the subcellular localization of SAMS genes was predicted using the BUSCA webserver [61].

4.2. Evolutionary Analysis

The amino acid sequences of all predicted SAMS proteins from the ten species were aligned by ClustalX, and a phylogenetic tree was constructed using the neighbor-joining method of Clustal Omega (<https://www.ebi.ac.uk/Tools/msa/clustalo/>). The phylogenetic tree was visualized using Evolview v3 server [62].

4.3. Conserved Motif Recognition

To identify the conserved motifs, the amino acid sequences of SAMS proteins were analyzed using the MEME v4.12.0 server (<http://meme-suite.org/tools/meme>) with the following parameters: motif width, between 6 and 50 residues; maximum number of motifs, 10 [63].

4.4. Prediction of Post-Translational and Post-Transcriptional Modification Sites

The phosphorylation sites among amino acid sequences of SAMS genes were predicted by the NetPhos 3.1 server (<http://www.cbs.dtu.dk/services/NetPhos/>) [64]. The N-glycosylation sites of SAMS proteins were predicted using the NetNGlyc 1.0 server (<http://www.cbs.dtu.dk/services/NetNGlyc/>) [65]. The threshold in NetPhos 3.1 and NetNGlyc 1.0 servers was set to a potential value >0.5. To predict the target sites of microRNA, the transcript sequences of selected SAMS genes were run against all published plant microRNAs using the psRNATarget server (<http://plantgrn.noble.org/psRNATarget/>) at an expectation level ≤ 2.5 [66].

4.5. Expression Profile Analysis Using RNA-Seq and Microarray Data

For the expression profiling of tomato SAMS genes, we utilized the 33 samples of published RNA-seq datasets that included transcription profiles of tomato fruit at four developmental stages (accession ID: E-MTAB-4818), root transcriptome profiles of chilling-sensitive tomato (*S. lycopersicum* cv. Moneymaker) and the cold-tolerant wild tomato (*S. habrochaites* LA1777) at optimal and suboptimal temperature (accession ID: E-MTAB-4855), transcriptome profiles of tomato shoot under biotic stress (*Pseudomonas syringae* pv. tomato DC3000) and red light treatment (accession GSE64087 of NCBI Sequence Read Archive database) [25], and low-temperature transcriptomes of *S. lycopersicum* and *S. habrochaites* [26]. The expression levels of tomato SAMS genes were normalized $((x-\mu)/sd)$ based on the published expression units, and a heatmap was constructed with the ‘*pheatmap*’ package of the R language. In addition, expression profiles of SAMS genes in *Arabidopsis thaliana* under different conditions and development stages were obtained from Affymetrix Arabidopsis ATH1 genome array (10,615 samples) using Genevestigator [45].

4.6. Plant Growth and Treatments

Seeds of *Solanum lycopersicum* cv. Moneymaker were sown in plates containing 60% vermicompost and 40% perlite and maintained under a 16 h photoperiod (5000 Lux) and a 24 ± 2 °C day/night temperature. After five weeks, healthy tomato seedlings were treated with different hormones and abiotic stresses. Treatments included brassinosteroid (BR) (5 μ M of epi-brassinosteroid), salicylic acid (SA) (30 mg/L), auxin (1 mg/L), abscisic acid (ABA) (10 mg/L), salt stress (150 mM of NaCl), cold stress (24 h at 8 °C), heat stress (24 h at 40 °C) and water stress. For the hormone treatments (BR, SA, ABA, and auxin), each hormone solution was sprayed onto the tomato seedlings at two times. After 6 h, whole shoots from each treatment were separately harvested and stored in liquid nitrogen at -80 °C. For the salt stress treatment, tomato seedlings were irrigated with a solution of 150 mM NaCl for two days. Whole shoots were harvested at the end of treatment. Cold and heat stresses were imposed by maintaining seedlings at 8 °C and 40 °C, respectively, for 24 h, and then the whole shoots were harvested. For the water stress treatment, irrigation was withheld for 10 days; whole shoots were then collected. Seedlings that had been maintained at 24 ± 2 °C were harvested as control samples. After applying the treatments, all collected samples of each treatment were immediately placed in liquid nitrogen and stored at -80 °C. All experimental treatments included three biological replicates.

4.7. RNA Extraction and qRT-PCR Analysis

The total RNA from the frozen samples was extracted using the RNX TM-Plus kit (Sinaclon, Iran) according to the manufacturer’s recommendations. The quantity and quality of the extracted RNA were analyzed using a Nano Photometer (Implen N50) and agarose gel electrophoresis. First-strand

complementary DNA (cDNA) was synthesized using 1 µg total RNA (treated with RNase-free DNase I (Thermo Fisher Scientific)) and reverse transcriptase (Roche, Germany) according to the manufacturers' protocols. The specific primers for the four tomato SAMS genes (Solyc12g099000, Solyc01g101060, Solyc09g008280, and Solyc10g083970) and EF-1- α (Solyc06g005060), as a reference gene, were designed using Primer3 Plus online software (Table S1). Real-time PCR was performed in 10 µl volumes using the Applied Biosystems StepOne™ system and RealQ Plus 2x Master Mix Green high ROX™ (Ampliqon) according to the instructions of the manufacturers. The real-time PCR conditions were as follows: 95 °C for 10 min, followed by 35 cycles at 95 °C for 15 s and 60 °C for 20 s. The melting curve for each sample was obtained after 35 cycles at the temperature range from 60 to 95 °C. The relative expression patterns of SAMS genes were calculated using the $2^{-\Delta\Delta Ct}$ method [67]. All graphs were constructed using Graphpad Prism 5.0 software based on the mean and standard deviation (SD) of the expression values of each gene.

5. Conclusions

In this study, members of the SAMS gene family were evaluated in several plant species, with focus on physiochemical properties, post-transcriptional and translational modifications, and expression patterns. The SAMS proteins varied in protein characterization features, conserved motifs, phylogenetic clustering analysis, post-translation modifications, and gene expression patterns. The tomato SAMS genes showed differential expression in response to stresses and hormone treatments. The various expression patterns of SAMS genes indicated that these genes play critical regulatory roles in metabolic pathways involved in the responses to environmental stresses. In addition, it seems that ABA and BR inhibit the ethylene and polyamines biosynthesis induced by SAMS genes. Our study provides very useful outputs and novel insights into the main roles of the SAMS gene family in plants. The overall results will be useful for future studies on the molecular functions of SAMS genes.

Supplementary Materials: The following are available online at <http://www.mdpi.com/2223-7747/9/5/586/s1>, Table S1: List of primers used for real-time PCR, Table S2: Putative miRNAs targeting the transcripts of SAMS genes at an expectation level < 4.00.

Author Contributions: Conceptualization, P.H.; Methodology, data analysis and validation, P.H., F.M. and T.N.; Project administration, P.H.; Writing, original draft, P.H. and T.N.; Writing, review and editing, P.H., T.N. and G.B. All authors have read and agreed to the published version of the manuscript.

Funding: This scientific publication was supported and partially funded by BreedOmics, the Laboratory service of Genomics for Breeding of the University of Padova, Italy.

Conflicts of Interest: The authors declare no conflict of interest.

References

1. Lu, S.C. S-adenosylmethionine. *Int. J. Biochem. Cell Biol.* **2000**, *32*, 391–395. [[CrossRef](#)]
2. Martínez-López, N.; Varela-Rey, M.; Ariz, U.; Embade, N.; Vazquez-Chantada, M.; Fernandez-Ramos, D.; Gomez-Santos, L.; Lu, S.C.; Mato, J.M.; Martinez-Chantar, M.L. S-adenosylmethionine and proliferation: New pathways, new targets. *Biochem. Soc. Trans.* **2008**, *36 Pt 5*, 848–852. [[CrossRef](#)]
3. Fontecave, M.; Atta, M.; Mulliez, E. S-adenosylmethionine: Nothing goes to waste. *Trends Biochem. Sci.* **2004**, *29*, 243–249. [[CrossRef](#)] [[PubMed](#)]
4. Chen, Y.; Zou, T.; McCormick, S. S-adenosylmethionine synthetase 3 is important for pollen tube growth. *Plant Physiol.* **2016**, *172*, 244–253. [[CrossRef](#)] [[PubMed](#)]
5. Sauter, M.; Moffatt, B.; Saechao, M.C.; Hell, R.; Wirtz, M. Methionine salvage and S-adenosylmethionine: Essential links between sulfur, ethylene and polyamine biosynthesis. *Biochem. J.* **2013**, *451*, 145–154. [[CrossRef](#)]
6. Wi, S.J.; Kim, W.T.; Park, K.Y. Overexpression of carnation S-adenosylmethionine decarboxylase gene generates a broad-spectrum tolerance to abiotic stresses in transgenic tobacco plants. *Plant Cell Rep.* **2006**, *25*, 1111–1121. [[CrossRef](#)] [[PubMed](#)]
7. Shen, B.; Li, C.; Tarczynski, M.C. High free-methionine and decreased lignin content result from a mutation in the Arabidopsis S-adenosyl-L-methionine synthetase 3 gene. *Plant J.* **2002**, *29*, 371–380. [[CrossRef](#)]

8. Bauerle, M.R.; Schwalm, E.L.; Booker, S.J. Mechanistic diversity of radical S-adenosylmethionine (SAM)-dependent methylation. *J. Biol. Chem.* **2015**, *290*, 3995–4002. [[CrossRef](#)]
9. Lin, S.; Shi, Q.; Nix, F.B.; Styblo, M.; Beck, M.A.; Herbin-Davis, K.M.; Hall, L.L.; Simeonsson, J.B.; Thomas, D.J. A Novel S-adenosyl-L-methionine: Arsenic (III) methyltransferase from rat liver cytosol. *J. Biol. Chem.* **2002**, *277*, 10795–10803. [[CrossRef](#)]
10. Lu, S.C.; Mato, J.M. S-adenosylmethionine in liver health, injury, and cancer. *Physiol. Rev.* **2012**, *92*, 1515–1542. [[CrossRef](#)]
11. Lee, H.-O.; Wang, L.; Kuo, Y.-M.; Andrews, A.J.; Gupta, S.; Kruger, W.D. S-adenosylhomocysteine hydrolase over-expression does not alter S-adenosylmethionine or S-adenosylhomocysteine levels in CBS deficient mice. *Mol. Genet. Metab. Rep.* **2018**, *15*, 15–21. [[CrossRef](#)] [[PubMed](#)]
12. He, Y.; Li, Y.; Chen, Y.; Feng, L.; Nie, Z. Homocysteine level and risk of different stroke types: A meta-analysis of prospective observational studies. *Nutr. Metab. Cardiovasc. Dis.* **2014**, *24*, 1158–1165. [[CrossRef](#)] [[PubMed](#)]
13. Chen, H.; Liu, S.; Ji, L.; Wu, T.; Ma, F.; Ji, Y.; Zhou, Y.; Zheng, M.; Zhang, M.; Huang, G. Associations between Alzheimer's disease and blood homocysteine, vitamin B12, and folate: A case-control study. *Curr. Alzheimer Res.* **2015**, *12*, 88–94. [[CrossRef](#)] [[PubMed](#)]
14. Alcázar, R.; Marco, F.; Cuevas, J.C.; Patron, M.; Ferrando, A.; Carrasco, P.; Tiburcio, A.F.; Altabella, T. Involvement of polyamines in plant response to abiotic stress. *Biotechnol. Lett.* **2006**, *28*, 1867–1876. [[CrossRef](#)]
15. Harpaz-Saad, S.; Yoon, G.M.; Mattoo, A.K.; Kieber, J.J. The formation of ACC and competition between polyamines and ethylene for SAM. In *Annual Plant Reviews Volume 44*; Wiley-Blackwell: Oxford, UK, 2012; pp. 53–81.
16. Bleecker, A.B.; Kende, H. Ethylene: A gaseous signal molecule in plants. *Annu. Rev. Cell Dev. Biol.* **2000**, *16*, 1–18. [[CrossRef](#)]
17. Chen, M.; Chen, J.; Fang, J.; Guo, Z.; Lu, S. Down-regulation of S-adenosylmethionine decarboxylase genes results in reduced plant length, pollen viability, and abiotic stress tolerance. *Plant Cell Tissue Organ Cult.* **2014**, *116*, 311–322. [[CrossRef](#)]
18. Wi, S.J.; Kim, S.J.; Kim, W.T.; Park, K.Y. Constitutive S-adenosylmethionine decarboxylase gene expression increases drought tolerance through inhibition of reactive oxygen species accumulation in Arabidopsis. *Planta* **2014**, *239*, 979–988. [[CrossRef](#)]
19. Roy, M.; Wu, R. Overexpression of S-adenosylmethionine decarboxylase gene in rice increases polyamine level and enhances sodium chloride-stress tolerance. *Plant Sci.* **2002**, *163*, 987–992. [[CrossRef](#)]
20. Hazarika, P.; Rajam, M.V. Biotic and abiotic stress tolerance in transgenic tomatoes by constitutive expression of S-adenosylmethionine decarboxylase gene. *Physiol. Mol. Biol. Plants* **2011**, *17*, 115–128. [[CrossRef](#)]
21. Espartero, J.; Pintor-Toro, J.A.; Pardo, J.M. Differential accumulation of S-adenosylmethionine synthetase transcripts in response to salt stress. *Plant Mol. Biol.* **1994**, *25*, 217–227. [[CrossRef](#)]
22. Li, X.-D.; Xia, B.; Wang, R.; Xu, S.; Jiang, Y.-M.; Yu, F.-B.; Peng, F. Molecular cloning and characterization of S-adenosylmethionine synthetase gene from *Lycoris radiata*. *Mol. Biol. Rep.* **2013**, *40*, 1255–1263. [[CrossRef](#)] [[PubMed](#)]
23. Mao, D.; Yu, F.; Li, J.; Van de Poel, B.; Tan, D.A.N.; Li, J.; Liu, Y.; Li, X.; Dong, M.; Chen, L. FERONIA receptor kinase interacts with S-adenosylmethionine synthetase and suppresses S-adenosylmethionine production and ethylene biosynthesis in Arabidopsis. *Plant Cell Environ.* **2015**, *38*, 2566–2574. [[CrossRef](#)] [[PubMed](#)]
24. Erb, T.J.; Evans, B.S.; Cho, K.; Warlick, B.P.; Sriram, J.; Wood, B.M.; Imker, H.J.; Sweedler, J.V.; Tabita, F.R.; Gerlt, J.A. A RubisCO-like protein links SAM metabolism with isoprenoid biosynthesis. *Nat. Chem. Biol.* **2012**, *8*, 926. [[CrossRef](#)] [[PubMed](#)]
25. Yang, Y.-X.; Wang, M.-M.; Yin, Y.-L.; Onac, E.; Zhou, G.-F.; Peng, S.; Xia, X.-J.; Shi, K.; Yu, J.-Q.; Zhou, Y.-H. RNA-seq analysis reveals the role of red light in resistance against *Pseudomonas syringae* pv. tomato DC3000 in tomato plants. *BMC Genom.* **2015**, *16*, 120. [[CrossRef](#)]
26. Chen, H.; Chen, X.; Chen, D.; Li, J.; Zhang, Y.; Wang, A. A comparison of the low temperature transcriptomes of two tomato genotypes that differ in freezing tolerance: *Solanum lycopersicum* and *Solanum habrochaites*. *BMC Plant Biol.* **2015**, *15*, 132. [[CrossRef](#)]
27. Heidari, P.; Ahmadizadeh, M.; Izanlo, F.; Nussbaumer, T. In silico study of the CESA and CSL gene family in Arabidopsis thaliana and Oryza sativa: Focus on post-translation modifications. *Plant Gene* **2019**, *19*, 100189. [[CrossRef](#)]

28. Bachmair, A.; Finley, D.; Varshavsky, A. In vivo half-life of a protein is a function of its amino-terminal residue. *Science* **1986**, *234*, 179–186. [[CrossRef](#)]
29. Kyte, J.; Doolittle, R.F. A simple method for displaying the hydropathic character of a protein. *J. Mol. Biol.* **1982**, *157*, 105–132. [[CrossRef](#)]
30. Ravanel, S.; Block, M.A.; Rippert, P.; Jabrin, S.; Curien, G.; Rébeillé, F.; Douce, R. Methionine metabolism in plants chloroplasts are autonomous for de novo methionine synthesis and can import s-adenosylmethionine from the cytosol. *J. Biol. Chem.* **2004**, *279*, 22548–22557. [[CrossRef](#)]
31. Ardito, F.; Giuliani, M.; Perrone, D.; Troiano, G.; Lo Muzio, L. The crucial role of protein phosphorylation in cell signaling and its use as targeted therapy. *Int. J. Mol. Med.* **2017**, *40*, 271–280. [[CrossRef](#)]
32. Friso, G.; van Wijk, K.J. Update: Post-translational protein modifications in plant metabolism. *Plant Physiol.* **2015**, *169*, 1469–1487. [[CrossRef](#)] [[PubMed](#)]
33. Silva-Sanchez, C.; Li, H.; Chen, S. Recent advances and challenges in plant phosphoproteomics. *Proteomics* **2015**, *15*, 1127–1141. [[CrossRef](#)] [[PubMed](#)]
34. Reddy, A.S.N.; Shad Ali, G. Plant serine/arginine-rich proteins: Roles in precursor messenger RNA splicing, plant development, and stress responses. *Wiley Interdiscip. Rev. RNA* **2011**, *2*, 875–889. [[CrossRef](#)] [[PubMed](#)]
35. Solá, R.J.; Griebenow, K. Effects of glycosylation on the stability of protein pharmaceuticals. *J. Pharm. Sci.* **2009**, *98*, 1223–1245. [[CrossRef](#)] [[PubMed](#)]
36. Schoberer, J.; Shin, Y.-J.; Vavra, U.; Veit, C.; Strasser, R. Analysis of Protein Glycosylation in the ER. In *The Plant Endoplasmic Reticulum*; Springer: Berlin, Germany, 2018; pp. 205–222.
37. Ding, J.; Zhou, S.; Guan, J. Finding microRNA targets in plants: Current status and perspectives. *Genom. Proteom. Bioinform.* **2012**, *10*, 264–275. [[CrossRef](#)] [[PubMed](#)]
38. Dong, H.; Lei, J.; Ding, L.; Wen, Y.; Ju, H.; Zhang, X. MicroRNA: Function, detection, and bioanalysis. *Chem. Rev.* **2013**, *113*, 6207–6233. [[CrossRef](#)]
39. Li, X.; Wang, X.; Zhang, S.; Liu, D.; Duan, Y.; Dong, W. Identification of soybean microRNAs involved in soybean cyst nematode infection by deep sequencing. *PLoS ONE* **2012**, *7*, e39650. [[CrossRef](#)]
40. Dong, Z.; Shi, L.; Wang, Y.; Chen, L.; Cai, Z.; Wang, Y.; Jin, J.; Li, X. Identification and dynamic regulation of microRNAs involved in salt stress responses in functional soybean nodules by high-throughput sequencing. *Int. J. Mol. Sci.* **2013**, *14*, 2717–2738. [[CrossRef](#)]
41. Devers, E.A.; Branscheid, A.; May, P.; Krajinski, F. Stars and symbiosis: MicroRNA-and microRNA*-mediated transcript cleavage involved in arbuscular mycorrhizal symbiosis. *Plant Physiol.* **2011**, *156*, 1990–2010. [[CrossRef](#)]
42. Cheah, B.H.; Jadhao, S.; Vasudevan, M.; Wickneswari, R.; Nadarajah, K. Identification of functionally important microRNAs from rice inflorescence at heading stage of a qDTY4. 1-QTL bearing Near Isogenic Line under drought conditions. *PLoS ONE* **2017**, *12*. [[CrossRef](#)]
43. Guo, W.; Wu, G.; Yan, F.; Lu, Y.; Zheng, H.; Lin, L.; Chen, H.; Chen, J. Identification of novel *Oryza sativa* miRNAs in deep sequencing-based small RNA libraries of rice infected with Rice stripe virus. *PLoS ONE* **2012**, *7*, e46443. [[CrossRef](#)]
44. Unver, T.; Tombuloglu, H. Barley long non-coding RNAs (lncRNA) responsive to excess boron. *Genomics* **2020**, *112*, 1947–1955. [[CrossRef](#)] [[PubMed](#)]
45. Hruz, T.; Laule, O.; Szabo, G.; Wessendorp, F.; Bleuler, S.; Oertle, L.; Widmayer, P.; Gruissem, W.; Zimmermann, P. Genevestigator v3: A reference expression database for the meta-analysis of transcriptomes. *Adv. Bioinform.* **2008**, *2008*, 420747. [[CrossRef](#)] [[PubMed](#)]
46. Ali, S.S.; Kumar, G.B.S.; Khan, M.; Doohan, F.M. Brassinosteroid enhances resistance to fusarium diseases of barley. *Phytopathology* **2013**, *103*, 1260–1267. [[CrossRef](#)] [[PubMed](#)]
47. Vishwakarma, K.; Upadhyay, N.; Kumar, N.; Yadav, G.; Singh, J.; Mishra, R.K.; Kumar, V.; Verma, R.; Upadhyay, R.G.; Pandey, M. Abscisic acid signaling and abiotic stress tolerance in plants: A review on current knowledge and future prospects. *Front. Plant Sci.* **2017**, *8*, 161. [[CrossRef](#)] [[PubMed](#)]
48. Singh, N.; Srivastava, S.; Shasany, A.K.; Sharma, A. Identification of miRNAs and their targets involved in the secondary metabolic pathways of *Mentha* spp. *Comput. Biol. Chem.* **2016**, *64*, 154–162. [[CrossRef](#)]
49. Huo, X.; Wang, C.; Teng, Y.; Liu, X. Identification of miRNAs associated with dark-induced senescence in *Arabidopsis*. *BMC Plant Biol.* **2015**, *15*, 266. [[CrossRef](#)]
50. Ahmadzadeh, M.; Heidari, P. Bioinformatics study of transcription factors involved in cold stress. *Biharean Biol.* **2014**, *8*, 83–86.

51. Heidari, P. Comparative Analysis of C-repeat Binding Factors (CBFs) in Tomato and Arabidopsis. *Braz. Arch. Biol. Technol.* **2019**, *62*. [[CrossRef](#)]
52. Wang, X.; Oh, M.W.; Komatsu, S. Characterization of S-adenosylmethionine synthetases in soybean under flooding and drought stresses. *Biol. Plant.* **2016**, *60*, 269–278. [[CrossRef](#)]
53. Sánchez-Aguayo, I.; Rodríguez-Galán, J.M.; García, R.; Torreblanca, J.; Pardo, J.M. Salt stress enhances xylem development and expression of S-adenosyl-L-methionine synthase in lignifying tissues of tomato plants. *Planta* **2004**, *220*, 278–285. [[CrossRef](#)] [[PubMed](#)]
54. Kumar, M.; Kumar, V.; Varma, A.; Prasad, R.; Sharma, A.K.; Pal, A.; Arshi, A.; Singh, J. An efficient approach towards the bioremediation of copper, cobalt and nickel contaminated field samples. *J. Soils Sediments* **2016**, *16*, 2118–2127. [[CrossRef](#)]
55. Serna, M.; Coll, Y.; Zapata, P.J.; Botella, M.Á.; Pretel, M.T.; Amorós, A. A brassinosteroid analogue prevented the effect of salt stress on ethylene synthesis and polyamines in lettuce plants. *Sci. Hortic. (Amsterdam)* **2015**, *185*, 105–112. [[CrossRef](#)]
56. Roje, S. S-Adenosyl-L-methionine: Beyond the universal methyl group donor. *Phytochemistry* **2006**, *67*, 1686–1698. [[CrossRef](#)]
57. Das, P.; Banerjee, A.; Roychoudhury, A. Polyamines Ameliorate Oxidative Stress by Regulating Antioxidant Systems and Interacting with Plant Growth Regulators. *Mol. Plant Abiotic Stress Biol. Biotechnol.* **2019**, *135–143*. [[CrossRef](#)]
58. Guo, Z.; Tan, J.; Zhuo, C.; Wang, C.; Xiang, B.; Wang, Z. Abscisic acid, H₂O₂ and nitric oxide interactions mediated cold-induced S-adenosylmethionine synthetase in *Medicago sativa* subsp. *falcata* that confers cold tolerance through up-regulating polyamine oxidation. *Plant Biotechnol. J.* **2014**, *12*, 601–612. [[CrossRef](#)]
59. Qi, Y.-C.; Wang, F.-F.; Zhang, H.; Liu, W.-Q. Overexpression of *suadea salsa* S-adenosylmethionine synthetase gene promotes salt tolerance in transgenic tobacco. *Acta Physiol. Plant.* **2010**, *32*, 263–269. [[CrossRef](#)]
60. Gasteiger, E.; Hoogland, C.; Gattiker, A.; Duvaud, S.; Wilkins, M.R.; Appel, R.D.; Bairoch, A. Protein identification and analysis tools on the ExPASy server. In *The Proteomics Protocols Handbook*; Humana Press: Totowa, NJ, USA, 2005; pp. 571–607.
61. Savojardo, C.; Martelli, P.L.; Fariselli, P.; Profiti, G.; Casadio, R. BUSCA: An integrative web server to predict subcellular localization of proteins. *Nucleic Acids Res.* **2018**, *46*, W459–W466. [[CrossRef](#)]
62. Subramanian, B.; Gao, S.; Lercher, M.J.; Hu, S.; Chen, W.-H. Evolvview v3: A webserver for visualization, annotation, and management of phylogenetic trees. *Nucleic Acids Res.* **2019**, *47*, W270–W275. [[CrossRef](#)]
63. Bailey, T.L.; Boden, M.; Buske, F.A.; Frith, M.; Grant, C.E.; Clementi, L.; Ren, J.; Li, W.W.; Noble, W.S. MEME SUITE: Tools for motif discovery and searching. *Nucleic Acids Res.* **2009**, *37*, W202–W208. [[CrossRef](#)]
64. Blom, N.; Gammeltoft, S.; Brunak, S. Sequence and structure-based prediction of eukaryotic protein phosphorylation sites. *J. Mol. Biol.* **1999**, *294*, 1351–1362. [[CrossRef](#)] [[PubMed](#)]
65. Gupta, R.; Brunak, S. Prediction of glycosylation across the human proteome and the correlation to protein function. *Pac. Symp. Biocomput.* **2002**, 310–322.
66. Dai, X.; Zhuang, Z.; Zhao, P.X. psRNATarget: A plant small RNA target analysis server (2017 release). *Nucleic Acids Res.* **2018**, *46*, W49–W54. [[CrossRef](#)] [[PubMed](#)]
67. Livak, K.J.; Schmittgen, T.D. Analysis of relative gene expression data using real-time quantitative PCR and the 2- $\Delta\Delta$ CT method. *Methods* **2001**, *25*, 402–408. [[CrossRef](#)]

